For publication in ***Proceedings of American Control Conference, June 2006, Minneapolis, Minnesota***

Life Extending Control of Mechanical Systems using Symbolic Time Series Analysis

Amol Khatkhate amk303@psu.edu
Shalabh Gupta szg107@psu.edu
Asok Ray axr2@psu.edu
Eric Keller eek105@psu.edu
Mechanical Engineering Department
The Pennsylvania State University
University Park, PA 16802
Corresponding Author: Asok Ray

***Abstract*— The paper presents *real-time* life extending control of complex mechanical structures based on the anomaly information generated via symbolic time series analysis. The underlying concept is experimentally validated on a multi-degree of freedom mass-beam structure excited by oscillatory motion of two shakers. The control policy is formulated based on the analysis of stochastic time series data of ultrasonic sensors collected under identical loading conditions. Experimental results demonstrate feasibility of the real-time control strategy for fatigue life extension of polycrystalline alloy structures.**

1. Introduction

The key idea of life extending control of mechanical structures is that substantial improvements in the useful service life of critical components can be achieved by insignificant reduction in the system dynamic performance (Ray et al. [1]). Zhang and Ray [2] and Zhang et al. [3] have demonstrated the efficacy of damage mitigation on a laboratory test apparatus, where intermittent overload pulses were deliberately injected as part of the feedforward control signal to cause crack retardation so that structural durability of critical structures is increased. However, damage-mitigation may not be meaningful unless the malignant anomalies leading to catastrophic failures are detected at an early stage.

Sole reliance on model-based analysis for structural damage monitoring is infeasible because of the difficulty in achieving requisite accuracy in modelling of fatigue damage evolution. Moreover, material uncertainties lead to stochastic nature of fatigue damage even under identical loading conditions [4]. The concept of symbolic time series analysis (STSA) [5] has been applied for early detection of slowly evolving anomalies [6] and a comparative evaluation of this novel analytical method shows its superior performance relative to other existing pattern recognition tools in terms of early detection of small changes in dynamical systems [7]. This paper reports how the information generated by symbolic time series analysis of ultrasonic data is utilized for early detection of fatigue damage in mechanical structures and is followed by the design of a control strategy for life extension of the stressed structures based on the analysis of stochastic data collected under identical experimental conditions.

A laboratory test apparatus has been constructed to experimentally validate the concepts of anomaly detection and life extending decision and control policies [2]. The test apparatus is designed to be sufficiently complex in itself due to partially correlated interactions amongst its individual components and functional modules. This paper focuses on ***real-time*** implementation and validation of anomaly detection method [6] and life extending control for enhancement of fatigue life in mechanical structures.

The paper is organized in seven sections including the present one. Section 2 briefly provides the description of the test apparatus used for experimental validation of anomaly detection and life extending control policy. Section 3 presents symbolic time series analysis method for anomaly detection and Section 4 discusses the life extending control strategy. Section 5 discusses the remaining life prediction methodology and section 6 presents the experimental results of real-time life extending control. Finally, the paper is concluded in section 7 with recommendations for future research.

2. Description of the Test Apparatus

With goal of investigating decision and control strategies for damage mitigation (i.e., life extension) in complex mechanical systems (e.g.,vehicular systems, power generation systems, and chemical plants), the test apparatus is designed to deliberately introduce fatigue damage in its critical component(s) (see Fig. 1 and Table I) [2]. These components are intentionally made to break in a reasonably short period of time to enhance the speed of conducting experiments. From these perspectives, the requirements of the test apparatus are:

- Operability under cyclic loading with multiple sources of input excitation.
- Damage accumulation in test specimens (at selected locations) within a reasonable period of time with negligible damage in other components of the test apparatus.

The test apparatus is designed and fabricated as a multi-degree of freedom (DOF) mass-beam structure excited by oscillatory motion of two vibrators as shown in Fig. 1. Physical dimensions of the pertinent components are listed in Table I. Two of the three major DOF's are directly controlled by the two actuators, Shaker #1 and Shaker #2, and the remaining

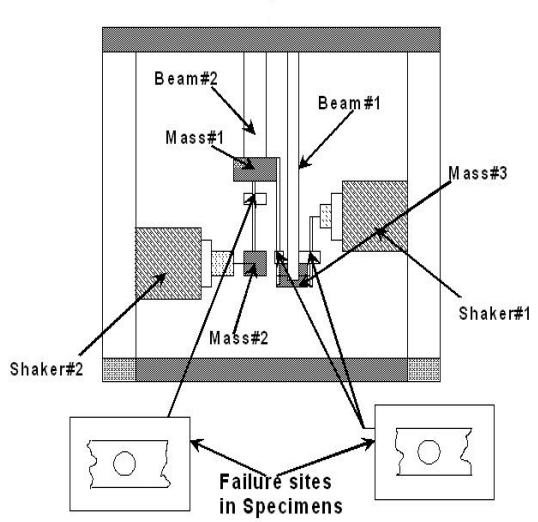

Fig. 1. Schematic Diagram for the Test Apparatus

TABLE I
STRUCTURAL DIMENSIONS OF THE TEST APPARATUS

Component	Material	Length (mm),Mass (kg) L x W x T
Mass 1	Mild Steel	2.82
Mass 2	Aluminium 6061-T6	0.615
Mass 3	Mild Steel	3.87
Beam 1	Mild Steel	800 x 22 x 11
Beam 2	Aluminium 6061-T6	711.2 x 22.2 x 11.1
3 Specimens	Aluminium 6061-T6	203.2 x 22.2 x 11.1

DOF is observable via displacement measurements of the three vibrating masses: Mass#1, Mass#2 and Mass#3. The inputs to the multivariable mechanical structure are the forces exerted by the two shakers; and the outputs to be controlled are the displacements of Mass#2 and Mass#3. The failure site in each specimen, attached to the respective mass is a circular hole (of radius 3.81mm) as shown in Fig. 1.

The test apparatus system is logically partitioned into two subsystems: (i) the plant subsystem consisting of the mechanical structure including the test specimens to undergo fatigue crack damage, actuators and sensors; and (ii) the instrumentation & control subsystem consisting of computers, data acquisition and processing, and communications hardware and software. Frequency of the reference signal is 14.69 Hz that is the resonating frequency associated with Mass#1 in the mechanical structure. The test specimens are thus excited by different levels of cyclic stress as two of them are directly affected by the vibratory inputs while the remaining one is subjected to resulting stresses, thus functioning as a coupling between the two vibrating systems. In the present configuration, three test specimens are identically manufactured and their material is 6061-T6 aluminum alloy. The software runs on the Real-Time Linux Operating System and is provided with A/D and D/A interfaces to the amplifiers serving the sensors and actuators of the test apparatus. The excitation signal is fed at the resonant frequency so as to facilitate the development of sufficient stress to break the specimens. The apparatus is equipped with *Ultrasonic Flaw Detectors* located on the specimen connecting Mass#1 and Mass#3 as seen in Fig. 2 for local damage sensing.

The sender and receiver ultrasonic transducers are placed on two positions, above and below the central notch, so as to send a sine wave signal at 5MHz through the region of crack propagation and receive it on the other side, as seen in Fig. 2. Since material characteristics (e.g., voids, dislocations and short cracks) influence the ultrasonic impedance, a small fault in the specimen is likely to change the signature of the signal at the receiver end. Therefore, the signal can be used to capture small changes during the early stages of fatigue damage, which may not be possible to detect by an optical microscope. It is observed that the crack always starts at the stress-concentrated region on the surface near the circular notch. There exists considerable scatter in fatigue data, and variations have been seen in the actual observed life of the specimens tested at same stress level. The scatter results as a consequence of fatigue sensitivity to a number of test and material parameters including specimen fabrication and surface preparation, metallurgical variables, specimen alignment in the apparatus, mean stress, and test frequency [8].

3. SYMBOLIC TIME SERIES ANALYSIS (STSA)

This section presents a brief description of Symbolic Time series Analysis (STSA) technique which has been recently developed and was reported by Ray in [6]. The symbolic dynamic analysis method takes advantage of the finite dimensional vector information generated by partitioning the available time series data in its wavelet domain. The steps are briefly described below in the following subsections:

A. Wavelet Space (WS) Partitioning

Several partitioning techniques have been reported in literature for symbol generation [9] [10] [11]. Recent literature has reported the wavelet-based partitioning approach [12] where wavelet transform [13] was shown to be particularly effective for noisy data from high-dimensional dynamical systems. In this method [6], the time series data is first converted to the wavelet transform data, where wavelet coefficients are generated at different scales and time shifts. The graphs of wavelet coefficients versus scale, at selected time shifts, are stacked starting with the smallest value of scale and ending with its largest value and then back from the largest value to the smallest value of the scale at the

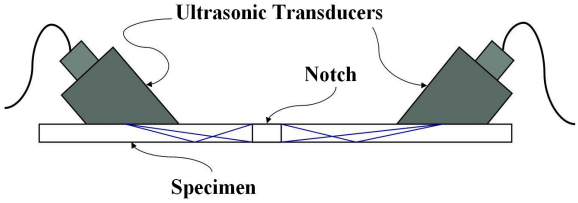

Fig. 2. Ultrasonic Flaw Detection scheme

next instant of time shift. The arrangement of the resulting *scale series* data in the wavelet space is then partitioned with alphabet size $|\mathcal{A}|$ by horizontal lines such that the regions with more information are partitioned finer and those with sparse information are partitioned coarser. In this approach, the maximum entropy is achieved by the partition that induces uniform probability distribution of the symbols in the symbol alphabet [12]. Shannon entropy is defined as

$$S = -\sum_{i=1}^{|\mathcal{A}|} p_i \; log(p_i) \tag{1}$$

where p_i is the probability of the i^{th} state and summation is taken over all possible states. Uniform probability distribution of states is a consequence of the maximum entropy partitioning. Also, this paper has utilized the absolute value of the scale series data points for partitioning because of the symmetry of data points about the mean position.

B. D-Markov Machine Construction

The partitioning as described in the previous sub-section is performed at time epoch t_0 of the nominal condition that is chosen to be a healthy condition having zero anomaly measure. A finite state machine is then constructed, where the states of the machine are defined corresponding to a given *alphabet* $\mathcal{A}$ and window length D. The alphabet size $|\mathcal{A}|$ is the total number of partitions while the window length D is the length of consecutive symbol words forming the states of the machine [6]. The states of the machine are chosen as all possible words of length D from the symbol sequence, thereby making the number n of states to be equal to the total permutations of the alphabet symbols within word of length D, (i.e., $n \leq |\mathcal{A}|^D$). The choice of $|\mathcal{A}|$ and D depends on specific experiments, noise level and also the available computation power. A large *alphabet* may be noise-sensitive while a small alphabet could miss the details of signal dynamics. Similarly, a high value of D is extremely sensitive to small signal distortions but would lead to larger number of states requiring more computation power. For details on choice of $\mathcal{A}$, refer [12]. For machine construction, the window of length D on the symbol sequence $\ldots \sigma_{i_1} \; \sigma_{i_2} \ldots \sigma_{i_k} \ldots$ is shifted to the right by one symbol, such that it retains the last (D-1) symbols of the previous state and appends it with the new symbol σ_{i_ℓ} at the end. The symbolic permutation in the current window gives rise to a new state. The machine constructed in this fashion is called D-Markov machine [6] because of its Markov properties.

Definition 3.1: A symbolic stationary process is called D-Markov if the probability of the next symbol depends only on the previous D symbols, i.e., $P(\sigma_{i_0}/\sigma_{i_{-1}}....\sigma_{i_{-D}}\sigma_{i_{-D-1}}....) = P(\sigma_{i_0}/\sigma_{i_{-1}}....\sigma_{i_{-D}})$.

The finite state machine constructed above has D-Markov properties because the probability of occurrence of symbol σ_{i_ℓ} on a particular state depends only on the configuration of that state, i.e., previous D symbols. For example, if $\mathcal{A} = \{0,1\}$, i.e., $|\mathcal{A}| = 2$ and $D = 2$, then the number of states is $n \leq |\mathcal{A}|^D = 4$; and the possible states are Q = {00, 01, 10, 11}, some of which may be forbidden, Fig. 3.

Once the partitioning alphabet $\mathcal{A}$ and word length D are determined at the nominal condition (time epoch t_0), they are kept constant for all (slow time) epochs $\{t_1, t_2, ...t_k....\}$, i.e. the structure of the machine is fixed at the nominal condition. The states of the machine are marked with the corresponding symbolic word permutation and the edges joining the states indicate the occurrence of an event σ_{i_ℓ}.

Definition 3.2: The probability of transitions from state q_j to state q_k belonging to the set Q of states under a transition $\delta : Q \times \mathcal{A} \rightarrow Q$ is defined as

$$\pi_{jk} = P(\sigma \in \mathcal{A} \mid \delta(q_j, \sigma) \rightarrow q_k); \sum_k \pi_{jk} = 1; \tag{2}$$

Thus, for a D-Markov machine, the irreducible stochastic matrix $\Pi \equiv [\pi_{ij}]$ describes all transition probabilities between states such that it has at most $|\mathcal{A}|^{D+1}$ nonzero entries. The left eigenvector $\mathbf{p}$ corresponding to the unit eigenvalue of Π is the state probability vector under the (fast time scale) stationary condition of the dynamical system [6]. On a given symbol sequence $....\sigma_{i_1}\sigma_{i_2}...\sigma_{i_l}....$ generated from the time series data collected at slow time epoch t_k, a window of length (D) is moved by keeping a count of occurrences of word sequences $\sigma_{i_1}\cdots\sigma_{i_D}\sigma_{i_{D+1}}$ and $\sigma_{i_1}\cdots\sigma_{i_D}$ which are respectively denoted by $N(\sigma_{i_1}\cdots\sigma_{i_D}\sigma_{i_{D+1}})$ and $N(\sigma_{i_1}\cdots\sigma_{i_D})$. Note that if $N(\sigma_{i_1}\cdots\sigma_{i_D}) = 0$, then the state $q \equiv \sigma_{i_1}\cdots\sigma_{i_D} \in Q$ has zero probability of occurrence. For $N(\sigma_{i_1}\cdots\sigma_{i_D}) \neq 0$, the transitions probabilities are then obtained by these frequency counts as follows.

$$\pi_{jk} = P[q_k|q_j] = \frac{P[q_k, q_j]}{P[q_j]} = \frac{P(\sigma_{i_1}\cdots\sigma_{i_D}\sigma_)}{P(\sigma_{i_1}\cdots\sigma_{i_D})} \approx \frac{N(\sigma_{i_1}\cdots\sigma_{i_D}\sigma_)}{N(\sigma_{i_1}\cdots\sigma_{i_D})} \tag{3}$$

where the corresponding states are denoted by $q_j \equiv \sigma_{i_1}\sigma_{i_2}\cdots\sigma_{i_D}$ and $q_k \equiv \sigma_{i_2}\cdots\sigma_{i_D}\sigma$.

The time series data under the nominal condition (set as a benchmark) generates the *state transition matrix* Π_{nom} that, in turn, is used to obtain the *state probability vector* p_{nom} whose elements are the stationary probabilities of the state vector, where $\mathbf{p}_{nom}$ is the left eigenvector of Π_{nom} corresponding to the (unique) unit eigenvalue.

C. Computation of Anomaly Measure

Subsequently, state probability vectors $\mathbf{p}_1, \; \mathbf{p}_2, \ldots \mathbf{p}_k....$ are obtained at slow-time epochs $t_1, t_2, \ldots t_k....$ based on the respective time series data. The behavioral changes from nominal condition are described as anomalies which are

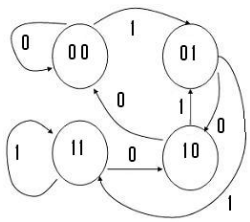

Fig. 3. Finite state automaton with D = 2 and $\mathcal{A} = \{0,1\}$

characterized by a scalar called *Anomaly Measure* ($\hat{\mathcal{M}}$). The anomaly measure is based on the following assumptions:

- Assumption 1: The evolution of damage is an irreversible process, i.e., with zero probability of self healing. This assumption implies the following conditions for all time t$\geq$ 0.
  i) $\hat{\mathcal{M}} \geq 0$;
  ii) $\frac{d\hat{\mathcal{M}}}{dt} \geq 0$
- Assumption 2: The damage accumulation at a slow time epoch t, when the dynamical system has reached a quasi-steady state equilibrium, is a function of the entire path taken to reach that state.

Let us digress in the context of fatigue damage. Although the crack length has been traditionally defined by a straight line joining the starting point to the tip of the crack, the actual crack follows a complicated path, possibly fractal in ductile materials, to reach a particular point. Therefore, the above assumption 2 implies that the anomaly measure should be determined from the actual path traversed and not just the end points. Accordingly, the path traversed $\mathcal{M}_k$ at a slow-time epoch t_k is defined as:

$$\mathcal{M}_k \equiv \mathcal{M}(t_k) \equiv \sum_{l=1}^{k} d\left(\mathbf{p}^l, \mathbf{p}^{l-1}\right);$$
$$d(\mathbf{x},\mathbf{y}) = \left(\sum_{j=1}^{|\mathcal{A}|} |x_j - y_j|^{\alpha} w(j)\right)^{\frac{1}{\alpha}} \tag{4}$$

where the exponent $\alpha \in [1,\infty)$ depends on the desired sensitivity to small deviations. Small changes in the signal profile, which might be due to noise and spurious oscillations in the signal, can be suppressed with large values of α. Therefore, the choice of α is a trade-off between suppression of small fluctuations due to noise and those due to the actual changes in the signal profile resulting from damage growth. In this application, the exponent is chosen to be $\alpha = 1.5$. Also, the weights $w(j)$ are chosen to be the squared mid-points of the respective partitioning levels such that higher levels are heavily weighted in order to capture small changes in the amplitude during the initial phases of fatigue damage. The relative distance travelled can be defined with respect to the point-to-point distance between starting point ($\mathbf{p}^0 \equiv$ uniform distribution obtained with maximum entropy partitioning) and final point ($\mathbf{p}^f \equiv \delta$-distribution with all the data points in the lowest partitioning level because of complete attenuation of the signal) to obtain the anomaly measure $\hat{\mathcal{M}}$ such that

$$\hat{\mathcal{M}}_k \equiv \hat{\mathcal{M}}(t_k) \equiv \frac{\sum_{l=1}^{k} d\left(\mathbf{p}^l, \mathbf{p}^{l-1}\right)}{d(\mathbf{p}^f, \mathbf{p}^0)} \tag{5}$$

The relative distance travelled from nominal to final point can be different for different specimens because of the stochastic nature of the fatigue damage. In order to avoid adding up spurious little fluctuations about some fixed point on the phase space the following algorithm is followed:

i) $\tilde{\mathbf{p}} = \mathbf{p}^0$;
ii) if $\left(\frac{d(\mathbf{p}^k, \tilde{\mathbf{p}})}{d(\mathbf{p}^f, \mathbf{p}^0)}\right) \geq \varepsilon$ then $I(\mathbf{p}^k, \tilde{\mathbf{p}}) = \frac{d(\mathbf{p}^k, \tilde{\mathbf{p}})}{d(\mathbf{p}^f, \mathbf{p}^0)}$; $\tilde{\mathbf{p}} = \mathbf{p}^k$;
else $I(\mathbf{p}^k, \tilde{\mathbf{p}}) = 0$;
iii) $\hat{\mathcal{M}}_k = \hat{\mathcal{M}}_{k-1} + I(\mathbf{p}^k, \tilde{\mathbf{p}})$;
iv) k = k + 1; Goto step ii;

where $\varepsilon = 0.01$ is chosen at the start of the ultrasonic instrument without starting load cycles. At this point measurement noise should not contribute to the anomaly measure and as such the anomaly measure must stay zero. This choice of ε eliminated the measurement noise and the increment in anomaly measure indicated progression of anomalies after the start of the experiment.

4. Proposed Life Extension Policy

The goal of life extending control is to detect the progression of malignant anomalies at an early stage and enable the system to take appropriate remedial action to circumvent damage. Also, control action should be delayed as far as possible so as to enable the system to perform at the desired level for maximum length of time.

The steps used in formulating the control policy are as follows and described in sections below :

1. Selection of anomaly measure threshold $\hat{\mathcal{M}}_{th}$ based on stochastic data of ultrasonic sensors collected under identical loading conditions.

2. Calculation of curvature ρ (i.e., change of slope) of anomaly measure plots after crossing the anomaly measure threshold $\hat{\mathcal{M}}_{th}$. A sharp curvature indicates transition from crack initiation to crack propagation phase.

3. Selection of curvature threshold ρ_{th} to decide the point of control action in *real-time*.

A. Selection of Anomaly Measure Threshold

Experiments were conducted under identical loading conditions (sinusoidal pulses with peak to peak amplitude of 18.8 V) to generate a stochastic data set of 10 identical samples as shown in Fig. 4. The threshold for anomaly measure is selected based on observation of the stochastic data. The anomaly measure value $\hat{\mathcal{M}}^*$ for each data set at the point of transition from crack initiation to crack propagation phase was recorded (see Fig. 5). The value of threshold $\hat{\mathcal{M}}_{th} = 0.15$ (see Fig. 4) was chosen with a conservative margin such that $\hat{\mathcal{M}}_{th} < min(\hat{\mathcal{M}}^*) = 0.1695$. This threshold provides an early warning of impending failure and one can soon expect a sharp deviation from the nominal behavior. At this point, small discontinuities and multiple short cracks have originated inside the specimen. Beyond this point, the behavior transits from short to long crack regime. The short crack regime is also evident by initial rise in the anomaly measure. This threshold also ensures that the control policy is robust to spurious effects during the initial short crack regime. This threshold allows the system to operate at the desired performance for maximum amount of time before the onset of widespread fatigue damage.

B. Selection of Curvature Threshold

After the crossover of the anomaly measure threshold $\hat{\mathcal{M}}_{th}$ in each sample of the stochastic data, curvature ρ_k was

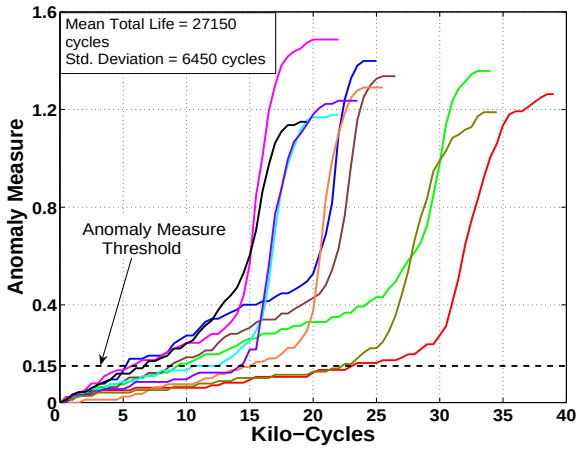

Fig. 4. Anomaly Measure plots for Stochastic Data of 10 similar specimens under identical loading

calculated at every time epoch t_k by the following equation

$$\begin{aligned}\rho_k &\equiv (\hat{\mathcal{M}}_k - \hat{\mathcal{M}}_{k-1}) - (\hat{\mathcal{M}}_{k-1} - \hat{\mathcal{M}}_{k-2}) \\ &= (\hat{\mathcal{M}}_k - 2\hat{\mathcal{M}}_{k-1} + \hat{\mathcal{M}}_{k-2}) \end{aligned} \quad (6)$$

The value of threshold $\rho_{th} = 0.024$ (see Fig. 5) was chosen such that $\rho_{th} < min(\rho^*) = 0.0243$. The point of control action is chosen at the time epoch where curvature threshold is reached indicating a transition from crack initiation to crack propagation phase. At this point, remaining life (with no control action) must be estimated (see Section 5) for a comparative evaluation with the observed life under the control action.

5. Remaining Life Prediction

The traditional approach to remaining life prediction is based on S-N curves of the test material. However, this approach is incapable of accurately identifying the rate at which fatigue cracks develop, and cannot be used for remaining life prediction in *real-time* [14]. Standard model based analysis [15] used to estimate fatigue crack growth rate are infeasible for real-time applications because of the stochastic nature of fatigue damage. Recently, stochastic modelling of fatigue crack propagation has been reported [16]. However, this model is based on long crack data and is incapable of issuing early warnings in the region of transitions from short crack to long crack regime. Therefore, this paper has utilized stochastic data collected from ultrasonic sensors which are capable of capturing evolving fatigue damage in the short crack regime. Also, the approach used in this paper takes advantage of the ***real-time*** computation of anomaly measure $\hat{\mathcal{M}}$ which is indicative of damage (relative to the initial nominal condition). At the point of control action, the remaining life can be estimated as follows :

$$\mathcal{R}_\rho = f(\hat{\mathcal{M}}, N);\ \hat{\mathcal{M}} >= 0,\ N >= 0 \quad (7)$$

where $\mathcal{R}_\rho$ is the expected remaining life at the point where ρ_{th} is crossed, $\hat{\mathcal{M}}$ is the corresponding anomaly measure and N is the used life at that time instant. The function is

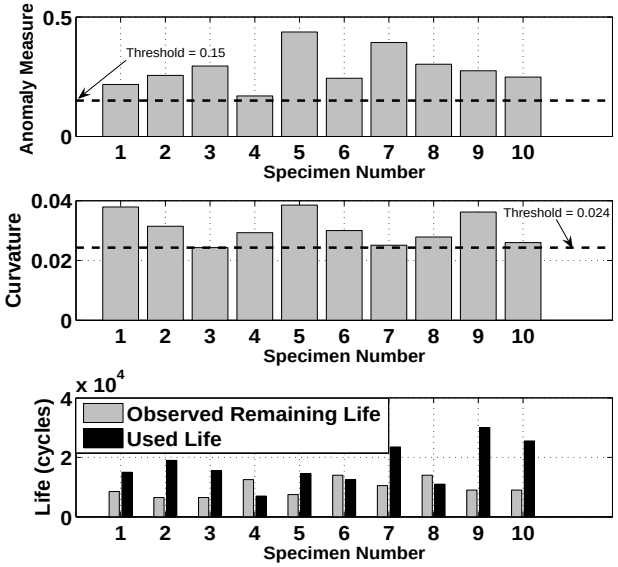

Fig. 5. These parameters are measured at the point curvature that, on the average, crosses the threshold of $\rho = 0.024$

assumed to be a quadratic (second-order) polynomial model of the form :

$$\mathcal{R}_\rho = a_0 + a_1\hat{\mathcal{M}} + a_2 N + a_3\hat{\mathcal{M}}^2 + a_4 N^2 + a_5\hat{\mathcal{M}}N \quad (8)$$

where the coefficients $a_i's$ are identified by least square multiple regression fit with the remaining life of the stochastic data (see Fig. 5) . The squared terms of the polynomial are called the quadratic effects and are used to model curvature in the response surface. The coefficients were identified as $a_0 = 1.155 \times 10^4$, $a_1 = 10.8 \times 10^4$, $a_2 = -2.03$, $a_3 = -21.16 \times 10^4$,$a_4 = 0.335 \times 10^{-4}$ and $a_5 = 1.876$. Fig. 6 shows the distribution of estimated and observed remaining life of the stochastic data.

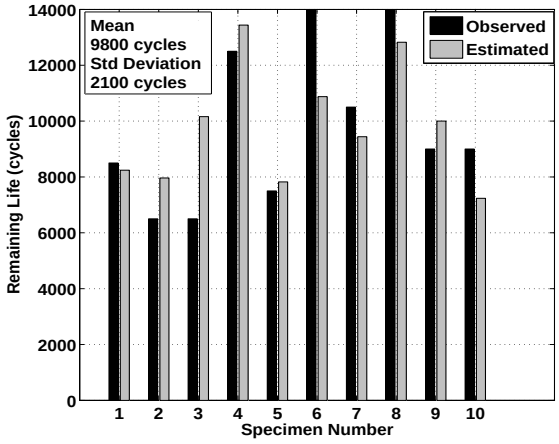

Fig. 6. Observed and Estimated Remaining Life after curvature threshold is crossed for 10 samples

6. Experimental Results and Discussion

This section presents the experimental results describing the effects of control action on structural durability, i.e., life of test specimens. Experiments were conducted at a sinusoidal load with peak to peak amplitude of 18.8 V to collect the stochastic data for off-line analysis. Based on the collected data for 10 samples, the specimens have an expected total life of 27150 cycles with a standard deviation of 6450 cycles. The proposed life extending methodology (described in Section 4) has been implemented on-line and the resulting ***real-time*** plots are shown in Fig. 7. For symbolic time series analysis (STSA) of the ultrasonic data, the finite state machine was constructed using alphabet size $|\mathcal{A}| = 8$, and depth $D = 1$. Increasing the value of $|\mathcal{A}|$ led to no further improvement in anomaly detection, and increasing the depth D created a large number of machine states, many of them having very small or zero probabilities. The finite state machine constructed with this choice of the parameters has only 8 states and was able to capture early anomalies. The wavelet basis function was chosen to be '*gaus2*' as it closely fits the sinusoidal signal [17].

The two plates in Fig. 7 represent the anomaly measure plots for experiments conducted on two identical specimens with different control actions (i.e., load reduction in the experiments that were taken in real time based on the control strategy in Section 4). The estimated life and the actual life after taking the control actions are presented in Table II. For total life calculation, experiments were stopped when the ultrasonic signal was completely attenuated upon breakage of the specimen. With 20 % load reduction, the percentage increase in life was about 108 % of the expected total life. Also, with 10 % load reduction, the increase in life amounted to about 32%. This observation also indicates that fatigue damage is a nonlinear and stochastic phenomenon because of the uncertainties involved in the material behavior. In-order to scale up the procedure to large scale structures, one needs to identify the important characteristics of the diagnosis curve and devise a control strategy accordingly.

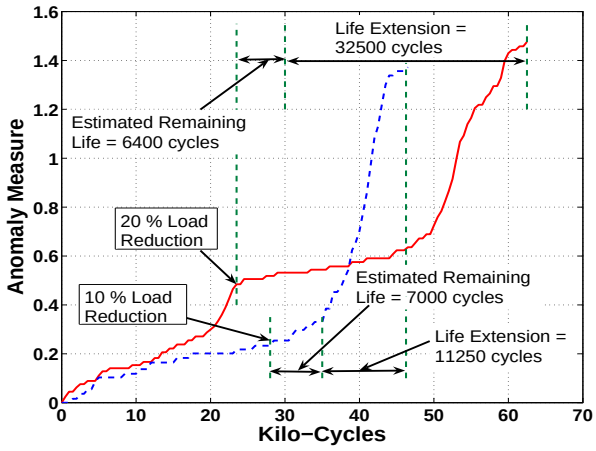

Fig. 7. Realtime Life Extension for two experiments with different levels of load reduction

TABLE II

Life Extension for different levels of load reduction

% Load Reduction	Used life N	Remaining life		Extended life (% total life)
		[1]Estimated	Observed	
10	28000	7000	18250	32
20	23500	6400	38900	108

4.The estimated remaining life is calculated at the point of control action based on the multiple regression fit obtained from stochastic data

7. Conclusions and Future Research

The *real-time* anomaly detection and life extending technique, presented in this paper, is built upon the principles of Symbolic Time Series Analysis (STSA). A life extending control policy has been successfully implemented in real time for different levels of load reduction to significantly increase the service life of the system. The following areas are recommended for future research.

- Validation of the symbolic time series method for early detection of fatigue damage in different materials with various geometries and loading conditions
- Design of adaptive and multiple control strategies to extend service life by larger magnitudes.

References

[1] A. Ray, M.-K.Wu, M. Carpino, and C. F. Lorenzo, Damage-Mitigating Control of Mechanical Systems: Parts I and II,*ASME J. Dyn. Syst., Meas., Control*,vol. 116, No. 3, 1994, pp 437-455.

[2] H. Zhang, A. Ray and S. Phoha, Hybrid Life Extending Control of Mechanical Systems: Experimental Validation of the Concept,*Automatica*, vol. 36, No. 1, 2000, pp 23-36.

[3] H. Zhang, and A. Ray, Robust Damage Damage-Mitigating Control of Mechanical Structures: Experimental Validation on a Test Apparatus,*ASME J. Dyn. Syst., Meas., Control*,, vol. 121, no. 3, 1999, pp 377-385.

[4] K. Sobczyk and B.F. Spencer, *Random Fatigue: Data to Theory*, Academic Press, Boston, MA., 1992.

[5] C.S. Daw and C.E.A. Finney and E.R. Tracy, A review of symbolic analysis of experimental data,*Review of Scientific Instruments*, vol.74,number 2, 2003,pp 915-930.

[6] A. Ray, Symbolic Dynamic Analysis of Complex Systems for Anomaly Detection, *Signal Processing*, vol. 84, no. 7, 2004, pp 1115-1130.

[7] S. Chin, A. Ray and V. Rajagopalan, Symbolic Time Series Analysis for Anomaly Detection: A Comparative Evaluation, *Signal Processing*, vol. 85, No. 9, 2005, pp 1859-1868.

[8] M. Klesnil and P. Lukas, *Fatigue of Metallic Materials*, Material Science Monographs 71, Elsevier, 1991.

[9] H.D.I. Abarbanel, *The Analysis of Observed Chaotic Data*, Springer-Verlag, New York, 1996.

[10] R.L. Davidchack, Y.C. Lai, E.M. Bolt and H. Dhamala, Estimating generating partitions of chaotic systems by unstable periodic orbits,*Physical Review E*, vol.61, 2000,pp 1353-1356.

[11] M.B. Kennel and M. Buhl, Estimating Good Discrete Partitions from Observed Data: Symbolic False Nearest Neighbors,*Physical Review E* vol. 91, no. 8, 2003, pp 084-102.

[12] V. Rajagopalan and A. Ray, "Wavelet-based Space partitioning for Symbolic Time Series Analysis", *Proceedings of 44th IEEE Conference on Decision and Control and European Control Conference*, Spain, Dec 2005.

[13] S. Mallat, *A Wavelet Tour of Signal Processing*, Academic Press, 1998.

[14] A.P. Parker, *The mechanics of fracture and fatigue*, London: E and F N Spon Ltd, 1981.

[15] P. Paris and F. Erdogan, A critical analysis of crack propagation laws,*Journal of Basic Engineering*, 1963, vol. 85, pp 528-534.

[16] A. Ray, Stochastic Modeling of Fatigue Crack Damage for Risk Analysis and Remaining Life Prediction, *Journal of Dynamic Systems, Measurement, and Control*, Trans. ASME, vol. 121, no. 3, pp 386-393.

[17] Wavelet Toolbox, MATLAB, Mathworks Inc.